International Journal of Industrial Innovation and Mechanical Engineering
Volume.1, No.4 November 2024
e-ISSN: 3047-4515, p-ISSN : 3047-4507, Page 23-31
DOI : https://doi.org/10.61132/ijiime.v1i4.52
Available online at: https://international.aritekin.or.id/index.php/IJIIME

Lossless Snubber-Based Bidirectional Full-Bridge Converter for Renewable Energy Applications

Qusay Jabbar Harjan[1*], Noora Salim[2]
[1]College of Science, Al-Qadisiyah University, Iraq
[2]Department of Water Resources Management Engineering- Al-Qasim Green University, Iraq
Email: qusay.harjan@qu.edu.iq [1], noora.salim@wrec.uoqasim.edu.iq [2]

*Corresponding author: qusay.harjan@qu.edu.iq**

Abstract. *In this study, we offer a new isolated bidirectional converter., which utilizes a novel snubber to provide soft switching for both primary switches without introducing additional energy losses to the snubber circuitry. The suggested converter has a low number of components and its control is simplified due to the fact that only one switch operates on each side. The performance of the proposed converter has been thoroughly analyzed and validated through simulation using PSPICE software, confirming the theoretical analysis of the converter.*

Keywords: *Bidirectional converter, Zero voltage switching, Lossless snubber, Isolated*

1. INTRODUCTION

The utilization of renewable energy sources has become more popular in recent decades as a means of lowering reliance on fossil fuels and reducing greenhouse gas emissions. Wind, solar, hydrogen fuel cell, and wave energy are some of the main renewable energy sources., and geothermal energy. Because renewable energy sources are unpredictable. The unpredictability of renewable energy sources means that their integration poses challenges in existing power systems. Bidirectional DC/DC converters are commonly used to increase or decrease the voltage level of renewable energy sources, such as solar panels, to the desired voltage level (boost mode) or to reduce the voltage level from high voltage side for battery storage (buck mode). The bidirectional dual-active bridge (DAB) DC/DC converter has gained significant attention in recent years due to its inherent characteristics. These bidirectional dc/dc converters and their variations are typically employed as an interface between the high and low voltage sides. They have a variety of applications, including functioning as an interface between renewable energy sources such as photovoltaic systems and energy storage batteries, as well as a dc link that transforms dc voltage to appropriate voltage and frequency for the grid via an inverter. These converters have different sections that researchers have focused on improving efficiency, high gain ratio, lower transformer turns ratio, power switch control method, low switching losses, and other related issues.

Received July 22,2024; Revised: August 26 ,2024; Accepted September 27, 2024; Online Available; September 30,2024

2. LITERATURE REVIEW

Proposed bidirectional converter

The proposed converter consists of two pairs of windings on two ferrite cores, with each winding placed on one side of the low voltage and high voltage. Leakage inductors LK1 and LK2, along with magnetizing inductors Lm1 and Lm2, are used to depict these windings. The auxiliary circuit includes capacitors Cr1 and Cr2, auxiliary diodes Da3, Da2, Da1, and Da4, and switches S2. Additionally, switches S1 handle the energy transfer from both sides. One of the main features of the converter is the isolation between the high voltage and low voltage sections, as well as the low number of switches and its simplified control.

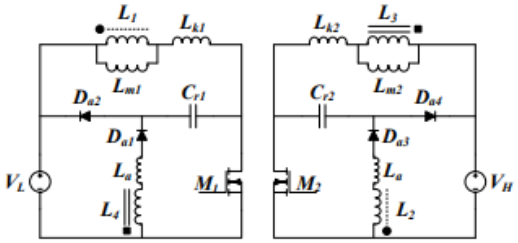

Figure 1 - Proposed isolated bidirectional converter

1-2 - Performance of the proposed bidirectional converter

The following assumptions have been made for simplicity in analyzing the converter:

- The output capacitors are sufficiently large, and their voltage remains constant throughout one cycle.
- The huge magnetizing inductors have a steady current flow.
- The semiconductor elements are ideal.

There are six operating modes for the suggested bidirectional converter.

The main waveforms of the converter are displayed in Figure 2, and the equivalent circuits fo r each mode of the converter are described in Figures 3 through 9.

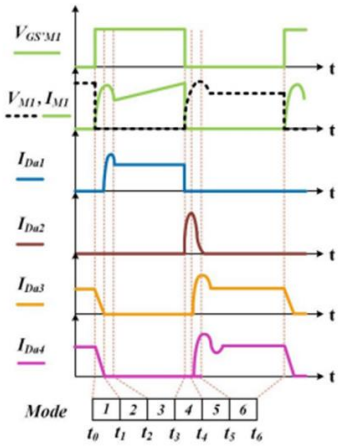

Figure 2 - Key waveforms of the proposed isolated bidirectional converter

first state:

This mode starts with the turning on of switch S1 while switch S2 is off. Because of the presence of a leakage inductor L, the switch current rises on a slope. As a result, the switch turns on in a zero-crossing (ZC) manner. At the same time, the current through diodes Da3 and Da4 linearly decreases until it reaches zero.

second state:

Resonance between Cr1 and L4 is created by turning off diodes Da3 and Da4,which transfers energy from Cr1 to inductor L4. This mode ends when the resonance current reaches zero. The output current in this mode is supplied by the output capacitor.

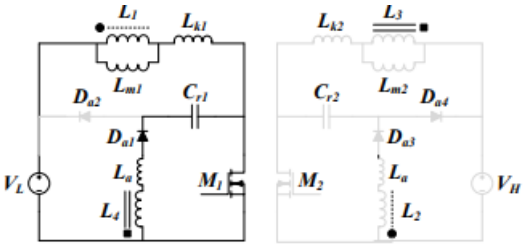

Figure 3: The suggested bidirectional converter's equivalent circuit for mode 2.

Third state:

In this mode, inductor Lm1 charges linearly with a slope of VLm1/Lm1, and diode Da4 is turned on. Energy from L4 is transferred to capacitor Cr2 through the coupling of L3-L4.

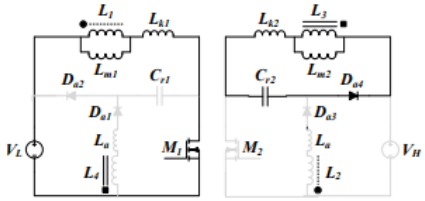

Figure 4 - Equivalent circuit of mode 3 of the proposed bidirectional converter

forth state:

This mode starts with the turning off of switch S1, and the magnetizing inductor current ILm1 starts to charge capacitor Cr1 linearly. The voltage across switch S1 reaches VL+Vcr1. Therefore, the turning off of S1 is in a zero-voltage (ZV) manner.

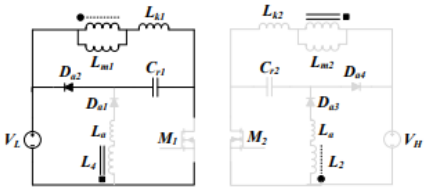

Figure 5 - Equivalent circuit for the fourth state of the proposed bidirectional converter.

State 5:

This case , all switches S1 , S2 off. Diodes Da3 ,Da4 on, and energy from inductor Lm1 is transferred to the output through these diodes and the coupling between L1-L2. Also, since the voltage across Cr2 resonates with Lk2, the switch voltage increases to the level of +Vcr2 and VL+Vcr1, and after half a cycle, it returns to the initial level.

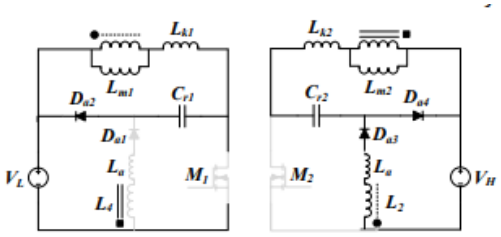

Figure 6 - Equivalent circuit for the fifth state of the proposed bidirectional converter.

State 6:

In this state, energy from inductor Lm1 is transferred to the output through the coupling between L1-L2 and diodes Da3 and Da4. This state ends when the switch S1 turns on.

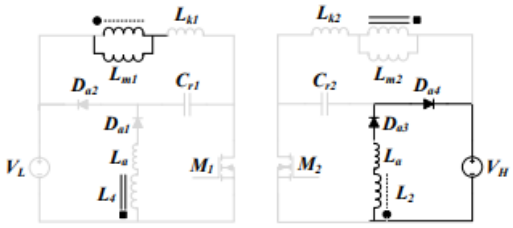

Figure 7 - Equivalent circuit for the sixth state of the proposed bidirectional converter.

It is worth mentioning that due to the complete symmetry of the converter in the sides with high and low voltages. the performance in the step-down mode is exactly similar to the step-up mode. Therefore, the description of it is omitted.

Examination of the suggested two-way converter

This section examines the efficiency and design of the proposed converter's inductor and snubber capacitors.

1-3 Efficiency of the suggested bidirectional converter.

In the steady-state condition, taking into account the leakage inductance effect when switch S1 is on, the voltage across inductors L1 and L2 can be obtained as follows.

1-4 $$V_{L1} = V_L \frac{L_{m1}}{L_{m1}+L_{k1}} DT$$

2-4 $$V_{L2} = -\frac{V_H}{n_a}(1-D)T$$

3-4 $$m = \frac{V_H}{V_L} = \frac{n_a D}{1-D} \times K$$

4 $$k = \frac{L_{m1}}{L_{m1}+L_{k1}}$$

If we neglect the leakage inductance compared to the magnetizing inductance, the efficiency simplifies as follows.

4-5 $$k = \frac{L_{m1}}{L_{m1}+L_{k1}}$$

5-5 $$n_a = \frac{\bar{N}_{a2}}{N_{a1}}$$

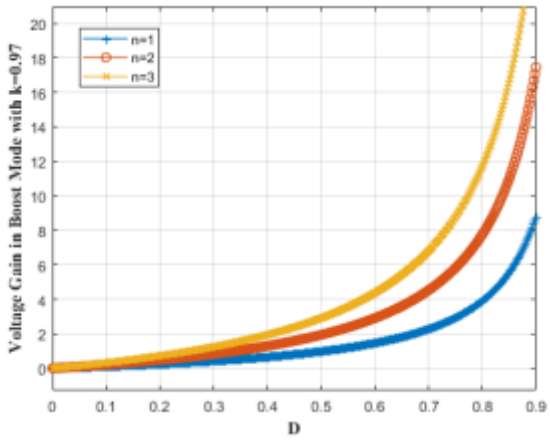

Figure 8 - Efficiency voltage waveform of the suggested bidirectional converter in the boosting mode plotted against duty cycle.

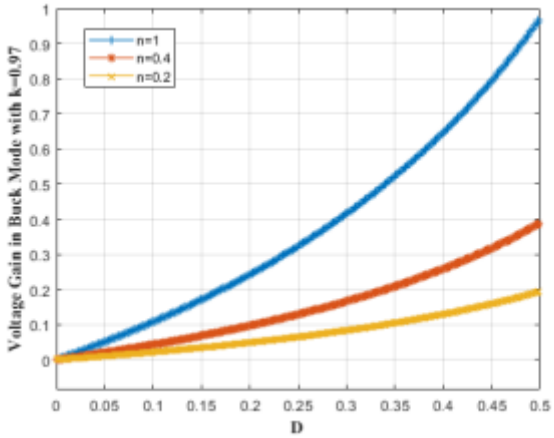

Figure 9 - Efficiency voltage waveform versus duty cycle of the proposed bidirectional converter in the bucking mode.

3. DISCUSSION

Simulation of the proposed highly efficient converter

Utilizing PSPICE software, to validate the study of the proposed converter, simulations were performed with an 80W power, 48V input, and 125V output voltage. Table 1 shows the specifications of the designed components. Figures 12 to 20 display the simulation results for both the boost and buck modes. The voltage and current waveforms of switch M1 in the boost mode simulation are shown in Figure 12. This picture illustrates how, when the switch is turned on, the current rises with a steep slope and zero-current switching conditions are reached for it.

When it turns off. Similarly, the voltage also rises with a steep slope when the switch turns off, indicating zero-voltage switching conditions for the switch. Figures 13 and 14 show the current waveforms of diodes Da1 and Da2. It can be observed that due to the diminishing current during turn-off, these diodes turn off with zero-current (ZC) switching and do not exhibit any reverse recovery problem. Therefore, they have negligible conduction losses. The current waveforms of diodes Da3 and Da4 in the high-side voltage in the boost mode are shown in figures 15 and 16. These diodes also turn on and off in a ZC manner and do not impose significant conduction losses on the converter. Figure 17 illustrates the simulated current and voltage waveforms of switch M2 in the buck mode. It is evident that this switch turns on in a zero-current switching (ZCS) manner and turns off in a zero-voltage switching (ZVS) manner. The current waveforms of diodes Da1 to Da4 in figures 18 to 21 are all turned off in a ZC manner and do not exhibit any reverse recovery problem.

Table 1 presents the specifications of the proposed converter and the values of its components.

Name of the piece	sign
V_{in}	48V
V_O	125V
Power switch	IRF740
L_1, L_2	200µH
Turns ratio=N	1
L_k	10µH
C_2-C_1	10nF
C_o	47µF
P_O	80W
f_S	100kHz

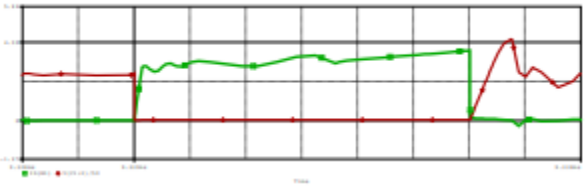

Figure 11: Current (green) and voltage (red) waveforms of switch 1 in the boost mode simulation.

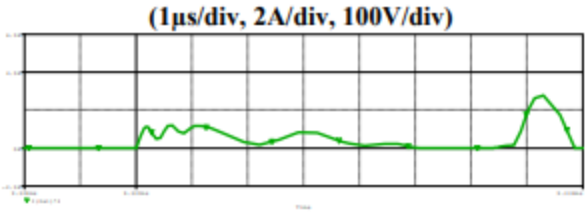

Figure 12: Current waveform of diode Da in the boost mode.

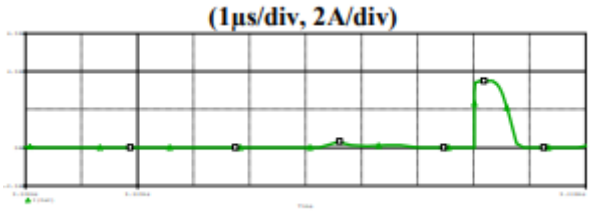

Figure 13: waveform of diode2 in the boost mode.

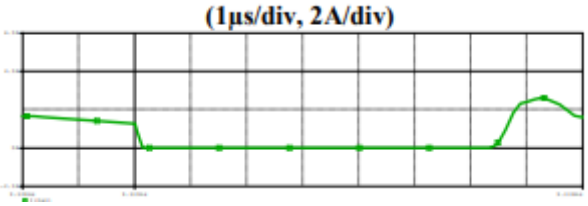

Figure 14: Current waveform of di Da3 in the mode simulation.

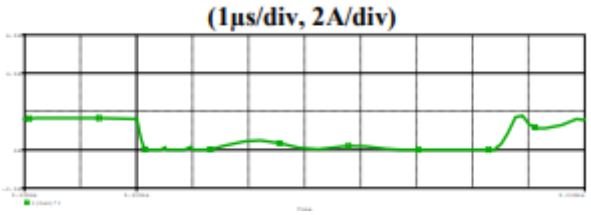

Figure 15 : Current waveform ofode Da4 in the mode simulation.

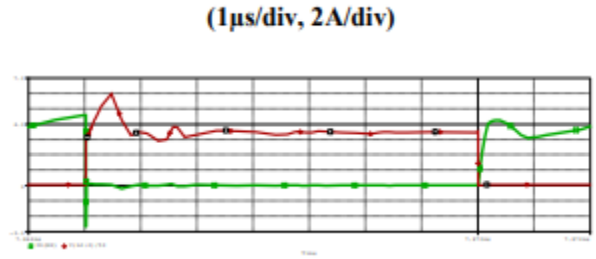

Figure 16: The current (green) and voltage (red) waveforms of switch M1 in the step-down mode, simulated on a scale.

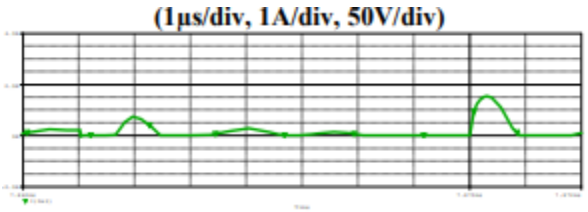

Figure 17: The current waveform of diode Da3 in the boost mode, simulated on a scale.

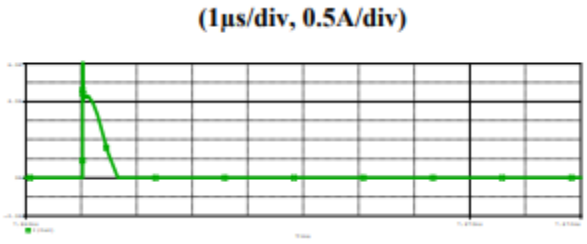

Figure 18: The current waveform of the diode in the boost mode, simulated on a scale.

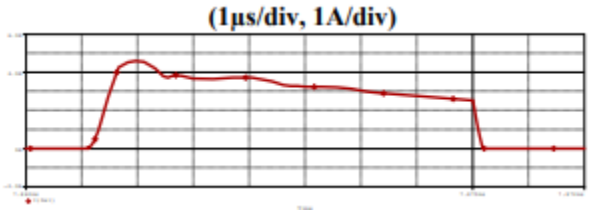

Figure 19: The current waveform of diode Da1 in the boost mode, simulated on a scale.

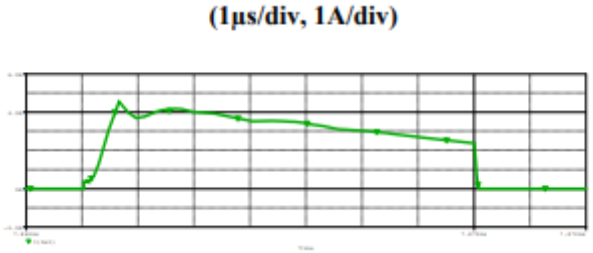

Figure 20: The current waveform of the diode in the boost mode, simulated on a scale.

4- A comparison of the strongly bucking and highly boosting modes of the suggested bidirectional converter efficiency. The efficiency of the suggested converter in both the bucking and boosting modes is displayed in Figure 22. The converter's efficiency decreases in both modes when power decreases because of the circulating current in the auxiliary circuit, and its maximum efficiency is attained at full load. Furthermore, the lack of easy switching conditions makes the efficiency decline more noticeable at light loads.

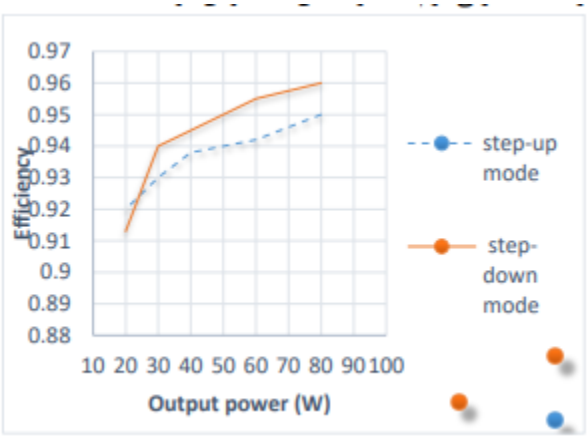

Figure 21. efficiency diagram of the proposed two-way converter in both highly increasing and highly decreasing modes

4. CONCLUSION

The advantages of the proposed converter can be categorized as follows:

- Providing ZCS (Zero Current Switching) conditions for the switches to turn on and ZVS (Zero Voltage Switching) conditions for them to turn off, thereby reducing switching losses.
- Turning off the body diodes using ZCS, solving the reverse recovery problem.
- Having a minimum possible number of auxiliary elements in the proposed bidirectional converter, resulting in reduced conduction losses.
- The PWM control of the proposed converter requires only one switch in each mode, simplifying the control circuit implementation.
- Energy transfer from the auxiliary circuit to the load in both the boosting and bucking modes.

REFERENCES

Cha, H., Chen, L., Ding, R., Tang, Q., & Peng, F. Z. (2018). An alternative energy recovery clamp circuit for full-bridge PWM converters with wide ranges of input voltage. *IEEE Transactions on Power Electronics*, 23(6), 2828–2837. https://doi.org/10.1109/TPEL.2017.2675386

Delshad, M., Asadi Madiseh, N., & Amini, M. R. (2013). Implementation of soft-switching bidirectional flyback converter without auxiliary switch. *IET Power Electronics*, 6(9), 1884–1891. https://doi.org/10.1049/iet-pel.2012.0396

Gu, B., Lai, J. S., Kees, N., & Zheng, C. (2017). Hybrid switching full-bridge DC-DC converter with minimal voltage stress of bridge rectifier, reduced circulating losses, and filter requirement for electric vehicle battery chargers. *IEEE Transactions on Power Electronics*, 28(3), 1132–1144. https://doi.org/10.1109/TPEL.2016.2637882

Lizhi, Z., Kunrong, W., Lee, F. C., & Sheng, L. J. (2000). New start-up schemes for isolated full-bridge boost converters. In *IEEE APEC 2000* (Vol. 1, pp. 309-313).

Murugan, M. (2014). Regulated bidirectional dc-to-dc voltage converter which maintains a continuous input current during step-up conversion. U.S. Patent No. 5,255,174.

Wang, K., Lee, F. C., & Lai, J. (1998). Bidirectional full-bridge dc/dc converter with unified soft-switching scheme, Part I: Principles of operation. In *Proc. VPEC Annu. Sem.* (pp. 143–149).

Zhu, L., Lai, J. S., & Lee, F. C. (2015). Accelerated commutation for passive clamp isolated boost converters. U.S. Patent No. 6,452,815.